

## Article

# Constraints on Graviton Mass from Schwarzschild Precession in the Orbits of S-Stars around the Galactic Center

Predrag Jovanović <sup>1,\*</sup>, Vesna Borka Jovanović <sup>2</sup>, Duško Borka <sup>2</sup> and Alexander F. Zakharov <sup>3</sup><sup>1</sup> Astronomical Observatory, Volgina 7, P.O. Box 74, 11060 Belgrade, Serbia<sup>2</sup> Department of Theoretical Physics and Condensed Matter Physics (020), Vinča Institute of Nuclear Sciences-National Institute of the Republic of Serbia, University of Belgrade, P.O. Box 522, 11001 Belgrade, Serbia; vborka@vinca.rs (V.B.J.); dusborka@vinca.rs (D.B.)<sup>3</sup> Bogoliubov Laboratory for Theoretical Physics, Joint Institute for Nuclear Research, 141980 Dubna, Russia; alex\_f\_zakharov5@mail.ru

\* Correspondence: pjovanovic@aob.rs

**Abstract:** In this paper we use a modification of the Newtonian gravitational potential with a non-linear Yukawa-like correction, as it was proposed by C. Will earlier to obtain new bounds on graviton mass from the observed orbits of S-stars around the Galactic Center (GC). This phenomenological potential differs from the gravitational potential obtained in the weak field limit of Yukawa gravity, which we used in our previous studies. We also assumed that the orbital precession of S-stars is close to the prediction of General Relativity (GR) for Schwarzschild precession, but with a possible small discrepancy from it. This assumption is motivated by the fact that the GRAVITY Collaboration in 2020 and in 2022 detected Schwarzschild precession in the S2 star orbit around the Supermassive Black Hole (SMBH) at the GC. Using this approach, we were able to constrain parameter  $\lambda$  of the potential and, assuming that it represents the graviton Compton wavelength, we also found the corresponding upper bound of graviton mass. The obtained results were then compared with our previous estimates, as well as with the estimates of other authors.

**Keywords:** theories of gravity; massive graviton; supermassive black hole; stellar dynamics.

**Citation:** Jovanović, P.; BorkaJovanović, V.; Borka, D.; Zakharov, A.F. Constraints on Graviton Mass from Schwarzschild Precession in the Orbits of S-Stars around the Galactic Center. *Symmetry* **2024**, *16*, 397. <https://doi.org/10.3390/sym16040397>

Academic Editors: Branko Dragovich, Vasilis K. Oikonomou and Sergei D. Odintsov

Received: 22 February 2024

Revised: 22 March 2024

Accepted: 26 March 2024

Published: 28 March 2024



**Copyright:** © 2024 by the authors. Licensee MDPI, Basel, Switzerland. This article is an open access article distributed under the terms and conditions of the Creative Commons Attribution (CC BY) license (<https://creativecommons.org/licenses/by/4.0/>).

## 1. Introduction

Here we use a phenomenological modification of the Newtonian gravitational potential with a non-linear Yukawa-like correction, as provided in [1,2], with the aim of obtaining new constraints on graviton mass from the observed orbits of S-stars around the Galactic Center.

The modified theories of gravity have been suggested as alternative approaches to Newtonian gravity in order to explain astrophysical observations at different astronomical and cosmological scales. There are a significant number of theories of modified gravity: [3–12].

Graviton is the gauge boson of the gravitational interaction and in GR theory is considered as massless, moving along null geodesics at the speed of light,  $c$ . On the other hand, according to a class of alternative theories, known as theories of massive gravity, gravitational interaction is propagated by a massive field, in which case graviton has some small non-zero mass [13–24]. This approach was first introduced in 1939 by Fierz and Pauli [13].

The LIGO and Virgo Collaborations considered a theory of massive gravity to be an appropriate approach and presented their estimate of the mass of the graviton,  $m_g < 1.2 \times 10^{-22}$  eV, in their first publication regarding gravitational wave detection from binary black holes [25]. Analyzing signals observed during the three observational runs collected in the third Gravitational-Wave Transient Catalog (GWTC-3), the LIGO–Virgo–KAGRA Collaborations obtained a stringer constraint of  $m_g < 1.27 \times 10^{-23}$  eV [26]. Various experimental constraints on the graviton mass are provided in [27].

There is a wide range of massive gravity theories, which have led to various phenomenologies [23]. However, several such models predict that gravitational potential in the Newtonian limit acquires a Yukawa suppression [23], so that the Poisson equation for Newtonian gravity,  $\nabla^2\Phi = 4\pi G\rho$ , is modified by graviton mass,  $m_g$ , and as noted in [28] it then takes the following form:

$$\left(\nabla^2 + \frac{1}{\lambda^2}\right)\Phi = 4\pi G\rho, \quad (1)$$

in which

$$\lambda = \frac{h}{m_g c} \quad (2)$$

is the Compton wavelength of the graviton. In such a case (see, e.g., [1,2,28]), the spherically symmetric potential,  $\Phi$ , of a body of mass  $M$  is provided by

$$\Phi(r) = -\frac{GM}{r} e^{-\frac{r}{\lambda}}. \quad (3)$$

Different Yukawa-like potentials are analyzed in papers [29–43], and more recently in [2,23,44–50]. As noted in [1], the exact form of the Yukawa-like potential,  $\Phi$ , should be, in principle, derived in the frame of a complete theory of massive gravity. Therefore, in our previous investigations we studied the case of massive gravity obtained from  $f(R)$  theories (see, e.g., [51–55]), which resulted in the Yukawa-like potential,  $\Phi$ , with two parameters: the range of Yukawa interaction,  $\Lambda$ , and its strength,  $\delta$ . In contrast, here we follow the approach from [1] and assume the above-mentioned particular phenomenology, according to which the potential,  $\Phi$ , takes the form of Equation (3), regardless of the theoretical model that produces it. As a consequence, we also assume that the metric at leading order in the Newtonian regime is (see, e.g., [56]) as follows:

$$ds^2 = \left(-1 + \frac{2GM}{c^2 r} e^{-\frac{r}{\lambda}}\right) c^2 dt^2 + \left(1 + \frac{2GM}{c^2 r} e^{-\frac{r}{\lambda}}\right) dl^2, \quad dl^2 \equiv dx^2 + dy^2 + dz^2. \quad (4)$$

Here, we study the trajectories of S-stars orbiting the central SMBH of our Galaxy, in the frame of Yukawa gravity using the modified PPN formalism [57–60]. Our present research is the continuation of our previous investigations of different extended gravity theories, where we used astrometric observations for S-star orbits [51–55,61–72].

The compact radio source Sgr A\* is very bright and located at the GC, while the so-called S-stars are the bright stars that move around it. The orbits of these S-stars around Sgr A\*, which was recently confirmed to be an SMBH (as was expected earlier [73–77]), have been monitored for approximately 30 years [78–96]. A number of analyses of S-star orbits have been performed using available observational data by some theoretical groups (see, e.g., [97–106]).

This paper is organized as follows: in Section 2, we present orbital precession in Yukawa-like gravitational potential. In Section 3, we introduce the PPN equations of motion, together with other important expressions we use for the analysis of stellar orbits around Sgr A\* in Yukawa gravity. We then perform an analysis of the potential from [2] that we previously developed for other modified potentials and obtain the results for the upper bound on graviton mass in the case of different S-stars. These results are presented and discussed in Section 4. Section 5 is devoted to the concluding remarks.

## 2. Orbital Precession in Yukawa-like Gravitational Potential

In order to derive the expression for orbital precession in gravitational potential (3), we assume that it does not differ significantly from the Newtonian potential,  $\Phi_N(r) = -\frac{GM}{r}$ . Namely, it is well known that orbital precession,  $\Delta\varphi$ , per orbital period, induced by small

perturbations to the Newtonian gravitational potential, which are described by the perturbing potential,  $V(r) = \Phi(r) - \Phi_N(r)$ , could be evaluated as (see, e.g., [65] and references therein)

$$\Delta\varphi^{rad} = \frac{-2L}{GMc^2} \int_{-1}^1 \frac{z \cdot dz}{\sqrt{1-z^2}} \frac{dV(z)}{dz}, \quad (5)$$

where  $r$  is related to  $z$  via  $r = \frac{L}{1+ez}$  and  $L = a(1-e^2)$  is the semilatus rectum of the orbital ellipse. An approximate formula for orbital precession,  $\Delta\varphi_Y$ , can be obtained by performing the power series expansion of the perturbing potential,  $V(r)$ , and by inserting the first-order term of this expansion into Equation (5), which results in

$$\Delta\varphi_Y^{rad} \approx \pi \sqrt{1-e^2} \frac{a^2}{\lambda^2}, \quad a \ll \lambda. \quad (6)$$

Note that a similar expression for orbital precession was obtained in [2], and it was used for bounding the Compton wavelength and mass of the graviton by the Solar System data.

### 3. Stellar Orbits in Extended/Modified PPN Formalisms

We simulated the orbits of S-stars around the GC using the Parameterized Post-Newtonian (PPN) equations of motion (for more details regarding the PPN approach, see, e.g., [107] and references therein). However, it is well known that Yukawa-like potentials could not be entirely represented by the standard PPN formalism and thus require its extension/modification (see the related references in [54]). This is also valid for the potential (3) and its corresponding metric (4). Moreover, since Yukawa gravity is indistinguishable from GR up to the first post-Newtonian correction [57], in addition to the standard PPN equations of motion,  $\vec{f}_{GR}$ , in GR, PPN equations of motion,  $\vec{f}_Y$ , in potential (3) also include an additional term,  $\vec{f}_\lambda$ , with exponential correction due to the perturbing potential,  $V(r)$ . In this extended PPN formalism (denoted here as PPN<sub>Y</sub>), the equations of motion are

$$\vec{f}_Y = \vec{f}_{GR} + \vec{f}_\lambda, \quad \vec{f}_{GR} = \vec{f}_N + \vec{f}_{PPN}, \quad (7)$$

where  $\vec{f}_N$  is the Newtonian acceleration,  $\vec{f}_{PPN}$  is the first post-Newtonian correction, and  $\vec{f}_\lambda$  is the additional Yukawa correction provided by the following expressions, respectively:

$$\begin{aligned} \vec{f}_N &= -GM \frac{\vec{r}}{r^3} \\ \vec{f}_{PPN} &= \frac{GM}{c^2 r^3} \left[ \left( 4 \frac{GM}{r} - \vec{r} \cdot \vec{r} \right) \vec{r} + 4(\vec{r} \cdot \vec{r}) \vec{r} \right] \\ \vec{f}_\lambda &= GM \left[ 1 - \left( 1 + \frac{r}{\lambda} \right) e^{-\frac{r}{\lambda}} \right] \frac{\vec{r}}{r^3}. \end{aligned} \quad (8)$$

The additional Yukawa correction,  $\vec{f}_\lambda$ , becomes negligible when  $\lambda \rightarrow \infty$ , and then  $\vec{f}_Y \rightarrow \vec{f}_{GR}$ , i.e., the PPN equations of motion,  $\vec{f}_Y$ , in potential (3) reduce to the standard PPN equations of motion in GR. Therefore, the orbits of S-stars in Yukawa gravity and GR can then be simulated by the numerical integration of the corresponding expressions (7).

The orbital precession in GR is provided by the well-known expression for the Schwarzschild precession [108],

$$\Delta\varphi_{GR}^{rad} \approx \frac{6\pi GM}{c^2 a(1-e^2)}, \quad (9)$$

where  $a$  is the semi-major axis and  $e$  is the eccentricity of the orbit. Recently, the GRAVITY Collaboration detected the orbital precession of the S2 star around the SMBH at the GC

and showed that it was close to the above prediction of GR [95]. For that purpose, they introduced an ad hoc factor,  $f_{SP}$ , in front of the first post-Newtonian correction of GR in order to parametrize the effect of the Schwarzschild metric. In this modified PPN formalism (denoted here as PPN<sub>SP</sub>), the equations of motion are provided by

$$\vec{r}_{SP} = \vec{r}_N + f_{SP} \cdot \vec{r}_{PPN}. \quad (10)$$

The corresponding modified expression for the Schwarzschild precession is [95]

$$\Delta\varphi_{SP}^{rad} = f_{SP} \cdot \Delta\varphi_{GR}^{rad}. \quad (11)$$

For  $f_{SP} = 1$ , expression (10) reduces to the standard PPN equations of motion,  $\vec{r}_{GR}$ , in GR provided in Equation (7), while expression (11) also reduces to the corresponding GR prediction from Equation (9). The parameter  $f_{SP}$  shows to what extent some gravitational models are relativistic, and it is defined as  $f_{SP} = (2 + 2\gamma - \beta)/3$ , where  $\beta$  and  $\gamma$  are the post-Newtonian parameters, and in the case of GR both of them are equal to 1 (and thus  $f_{SP} = 1$  in this case). For  $f_{SP} = 0$ , the Newtonian case is recovered. However, in the case of the S2 star a value of  $f_{SP} = 1.10 \pm 0.19$  was obtained by the GRAVITY Collaboration, indicating the orbital precession of  $f_{SP} \times 12.1$  in its orbit around Sgr A\* [95]. Recently, this collaboration updated the above first estimate to  $f_{SP} = 0.85 \pm 0.16$ , also obtained from the detected Schwarzschild precession of the S2 star's orbit [109]. Furthermore, they also presented the following estimate obtained from the fit with the four-star (S2, S29, S38, S55) data with the  $1\sigma$  uncertainty:  $f_{SP} = 0.997 \pm 0.144$  [109].

#### 4. Results: Constraints on the Compton Wavelength and Mass of the Graviton

The constraints on parameter  $\lambda$ , under which the orbital precession in the gravitational potential (3) deviates from the Schwarzschild precession in GR by a factor  $f_{SP}$ , can be obtained provided that the total orbital precession in Yukawa gravity, provided by the sum  $\Delta\varphi_{GR} + \Delta\varphi_Y$ , is close to the observed precession,  $\Delta\varphi_{SP}$ , obtained by the GRAVITY Collaboration:

$$\Delta\varphi_Y + \Delta\varphi_{GR} \approx \Delta\varphi_{SP} \Leftrightarrow \pi\sqrt{1-e^2}\frac{a^2}{\lambda^2} + \frac{6\pi GM}{c^2 a(1-e^2)} \approx f_{SP} \frac{6\pi GM}{c^2 a(1-e^2)}. \quad (12)$$

Taking into account the third Kepler law (since the orbits are almost Keplerian),

$$\frac{P^2}{a^3} \approx \frac{4\pi^2}{GM}, \quad (13)$$

then from Equations (12) and (13) one can obtain the following relation between  $\lambda$  and  $f_{SP}$ :

$$\lambda(P, e, f_{SP}) \approx \frac{cP}{2\pi} \frac{(1-e^2)^{\frac{3}{4}}}{\sqrt{6(f_{SP}-1)}}, \quad f_{SP} > 1. \quad (14)$$

The above condition can be used for constraining the Compton wavelength,  $\lambda$ , of the graviton by the observed values of  $f_{SP}$  only in cases when  $f_{SP}$  is larger than 1, since  $\Delta\varphi_Y$  always provides a positive contribution to the total precession in Equation (12). The corresponding constraints on the graviton mass,  $m_g$ , can then be found by inserting the obtained value of  $\lambda$  into Equation (2). The relative error of parameter  $\lambda$  (and thus of the graviton mass,  $m_g$ ) in this case can be found by differentiating the logarithm of the above expression (14):

$$\frac{|\Delta\lambda|}{\lambda} = \frac{|\Delta m_g|}{m_g} \leq \left( \frac{|\Delta P|}{P} + \frac{3e|\Delta e|}{2(1-e^2)} + \frac{|\Delta f_{SP}|}{2(f_{SP}-1)} \right). \quad (15)$$

It can be seen that potential (3) results in the same relative errors as the corresponding Yukawa potential derived in the frame of  $f(R)$  theories of gravity (see, e.g., [55]).

We first used three estimates for  $f_{SP}$ , obtained by the GRAVITY Collaboration, in order to find the corresponding constraints on the Compton wavelength,  $\lambda$ , of the graviton and its mass,  $m_g$ , in the case of the S2 star. These are the values of  $f_{SP}$  detected by GRAVITY collaboration in the case of S2 star [95,109], as well as from the combination of a few other stars: S2, S29, S38, and S55 [109]. For two estimates that were lower than 1, we used the upper limits of their  $1\sigma$  intervals, i.e., the values  $f_{SP} + \Delta f_{SP}$ . The obtained constraints are provided in Table 1, from which it can be seen that the most reliable result was obtained in the case of  $f_{SP}$  with the lowest uncertainty, resulting from the fit with the four-star data. In that case, the relative error for  $\lambda$  and  $m_g$  was the lowest. In contrast, the worst constraint with an unrealistically high relative error was obtained in the second case with the lowest value of  $f_{SP} = 1.01$ , due to the fact that it is too close to the corresponding prediction of GR. By comparing the results obtained in the first case with our previous corresponding estimates from Table I in [55], obtained for Yukawa-like potential derived from  $f(R)$  theories of gravity, it can be seen that the upper bound on graviton mass,  $m_g$ , and its absolute error,  $\Delta m_g$ , were improved by  $\sim 30\%$  in the case of the phenomenological potential (3), although the relative error remained the same.

**Table 1.** The Compton wavelength of the graviton,  $\lambda$ , and its mass,  $m_g$ , as well as their relative and absolute errors, calculated for three different values of  $f_{SP}$  in the case of the S2 star.

$f_{SP}$	$\Delta f_{SP}$	$\lambda \pm \Delta\lambda$ (AU)	$m_g \pm \Delta m_g$ ( $10^{-24}$ eV)	R.E. (%)
1.100	0.190	66361.5 $\pm$ 63890.7	124.9 $\pm$ 120.2	96.3
1.010	0.160	209853.4 $\pm$ 1681506.5	39.5 $\pm$ 316.5	801.3
1.141	0.144	55886.4 $\pm$ 29251.3	148.3 $\pm$ 77.6	52.3

In the first case of  $f_{SP} = 1.10 \pm 0.19$ , we also graphically compared the simulated orbits of the S2 star, obtained by the numerical integration of the equations of motion in the PPN<sub>SP</sub> formalism provided by Equation (10), with those in the PPN<sub>Y</sub> formalism provided by Equation (7) for  $\lambda = 66361.5$  AU, which corresponds to this  $f_{SP}$  according to Equation (14). The comparisons during one and five orbital periods are presented in the top-left and bottom-left panels of Figure 1, respectively, while in the corresponding right panels we present the differences between the corresponding  $x$  and  $y$  coordinates in these two PPN formalisms as the functions of time. In order to see more clearly the difference between the simulated orbits of the S2 star in two PPN formalisms, we show in the middle panel of Figure 1 part of its orbit near the pericenter (left panel) and near the apocenter (right panel).

As can be seen from Figure 1, the differences between the simulated orbits of the S2 star in these two PPN formalisms are very small, and the maximum discrepancy between the corresponding coordinates during the first orbital period is only  $\sim 2$  AU at the pericenter. This discrepancy slowly increases with time during the successive orbital periods due to neglecting the higher-order terms in the power-series expansion of the perturbing potential,  $V(r)$ , in Equation (5). One should also note that the two PPN formalisms provide close, but not exactly the same, epochs of pericenter passage, as can be seen from the top-right panel of Figure 1.

This sufficiently small difference between the simulated orbits in the two studied PPN formalisms confirms that relation (14) could be used for obtaining the constraints on the Compton wavelength,  $\lambda$ , of the graviton and its mass,  $m_g$ , from the latest estimates for  $f_{SP}$  obtained by the GRAVITY Collaboration.

Taking the above considerations into account, we then estimated the Compton wavelength,  $\lambda$ , of the graviton, its mass,  $m_g$ , and also their relative and absolute errors for all S-stars from Table 3 in [85], except for the S111 star. For that purpose, and in order to avoid the cases when  $f_{SP} < 1$ , we adopted the same strategy as in [55] and assumed that the recent GRAVITY estimates for  $f_{SP}$  are very close to the value in GR of  $f_{SP} = 1$ ,

so that these estimates represent a confirmation of GR within  $1\sigma$ . Therefore, we constrained the graviton mass,  $m_g$ , in the particular cases when  $f_{SP} = 1 + \Delta f_{SP} \pm \Delta f_{SP}$ , i.e., for  $f_{SP} = 1.19 \pm 0.19$ ,  $f_{SP} = 1.16 \pm 0.16$ , and  $f_{SP} = 1.144 \pm 0.144$ . As before, we used the expressions (14), (15), and (2) for this purpose, and the obtained results are presented in Tables 2 and 3. Furthermore, Table 2 also contains the results for  $f_{SP} = 1.10 \pm 0.19$  since, as shown in Table 1, this estimate is sufficiently larger than 1.

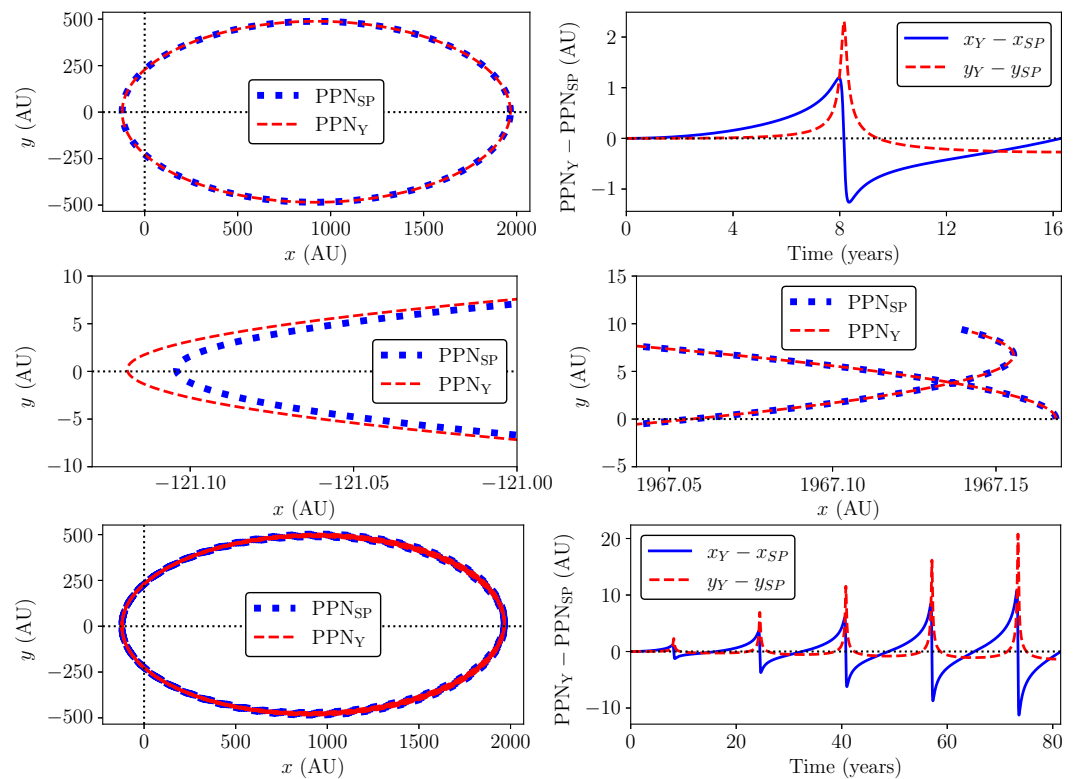


**Figure 1.** **Top left:** Comparison between the simulated orbits of the S2 star during one orbital period, obtained by numerical integration of the equations of motion provided by Equation (10) in the  $PPN_{SP}$  formalism for  $f_{SP} = 1.10$  (blue dotted line) and those provided by Equation (7) in the  $PPN_Y$  formalism for  $\lambda = 66361.5$  AU (red dashed line), which corresponds to  $f_{SP} = 1.10$  according to Equation (14). **Top right:** The differences between the corresponding  $x$  and  $y$  coordinates in the  $PPN_Y$  and  $PPN_{SP}$  formalisms as the functions of time. **Middle:** Comparison between the simulated orbits of the S2 star, near pericenter (**left**) and near apocenter (**right**) in two PPN formalisms. **Bottom:** The same as in the top panel, but for five orbital periods.

Using data from these tables, in Figure 2 we provide the comparison of the estimated Compton wavelength,  $\lambda$ , of the graviton, as well as for the graviton mass upper bound, for four stars (S2, S29, S38, S55), which the GRAVITY Collaboration used for the newest estimation of  $f_{SP}$ . As can be seen from Figure 2, all constraints in the case of the S2, S38, and S55 stars are approximately of the same order of magnitude ( $\lambda \sim 10^5$  AU and  $m_g \sim 10^{-22}$  eV). The only exception is the S29 star since it results with an order of magnitude larger values of  $\lambda$ , and hence an order of magnitude smaller than estimates for the upper bound on graviton mass,  $m_g$ . This is not surprising because the S29 star has a much longer orbital period of  $\sim 101$  yrs. with respect to the orbital periods of the other three stars, which are  $\sim 13$ – $20$  yrs. (see Table 3 from [85]).

If one compares these results with our previous corresponding estimates from Tables I and III in [55], obtained for Yukawa-like potential derived from  $f(R)$  theories of gravity, it can be noticed that both the upper bound on graviton mass,  $m_g$ , and its absolute error in the case of Yukawa-like potential (3) were further improved by  $\sim 30\%$ , in a similar way as for the S2 star in the first case from Table 1 (i.e., for  $f_{SP} = 1.10 \pm 0.19$ ).

**Table 2.** The Compton wavelength of the graviton,  $\lambda$ , and its mass,  $m_g$ , as well as their relative and absolute errors, calculated for  $f_{SP} = 1.10 \pm 0.19$  and  $f_{SP} = 1.19 \pm 0.19$  in the case of all S-stars from Table 3 in [85], except for S111.

Star	$f_{SP} = 1.1 \pm 0.19$			$f_{SP} = 1.19 \pm 0.19$		
	$\lambda \pm \Delta\lambda$ (AU)	$m_g \pm \Delta m_g$ ( $10^{-24}$ eV)	R.E. (%)	$\lambda \pm \Delta\lambda$ (AU)	$m_g \pm \Delta m_g$ ( $10^{-24}$ eV)	R.E. (%)
S1	1.6e+06 ± 1.6e+06	5.1 ± 5.1	100.7	1.2e+06 ± 6.6e+05	7.0 ± 3.9	55.7
S2	6.6e+04 ± 6.4e+04	124.9 ± 120.2	96.3	4.8e+04 ± 2.5e+04	172.1 ± 88.3	51.3
S4	8.8e+05 ± 8.5e+05	9.4 ± 9.1	96.7	6.4e+05 ± 3.3e+05	13.0 ± 6.7	51.7
S6	1.0e+06 ± 9.5e+05	8.3 ± 7.9	95.2	7.2e+05 ± 3.6e+05	11.5 ± 5.8	50.2
S8	5.5e+05 ± 5.4e+05	15.0 ± 14.7	98.0	4.0e+05 ± 2.1e+05	20.6 ± 10.9	53.0
S9	4.5e+05 ± 4.4e+05	18.6 ± 18.6	99.7	3.2e+05 ± 1.8e+05	25.7 ± 14.0	54.7
S12	2.4e+05 ± 2.3e+05	34.9 ± 33.6	96.4	1.7e+05 ± 8.9e+04	48.1 ± 24.7	51.4
S13	5.5e+05 ± 5.2e+05	15.1 ± 14.5	95.5	4.0e+05 ± 2.0e+05	20.9 ± 10.5	50.5
S14	7.3e+04 ± 7.8e+04	114.1 ± 122.4	107.3	5.3e+04 ± 3.3e+04	157.2 ± 98.0	62.3
S17	8.7e+05 ± 8.5e+05	9.5 ± 9.2	97.1	6.3e+05 ± 3.3e+05	13.1 ± 6.8	52.1
S18	4.5e+05 ± 4.3e+05	18.4 ± 17.8	96.5	3.3e+05 ± 1.7e+05	25.4 ± 13.1	51.5
S19	9.4e+05 ± 1.1e+06	8.8 ± 10.2	116.4	6.8e+05 ± 4.9e+05	12.1 ± 8.7	71.4
S21	2.5e+05 ± 2.5e+05	33.3 ± 33.2	99.6	1.8e+05 ± 9.9e+04	45.9 ± 25.1	54.6
S22	5.9e+06 ± 6.7e+06	1.4 ± 1.6	114.1	4.3e+06 ± 3.0e+06	1.9 ± 1.3	69.1
S23	4.5e+05 ± 5.2e+05	18.5 ± 21.4	115.6	3.2e+05 ± 2.3e+05	25.5 ± 18.0	70.6
S24	1.3e+06 ± 1.3e+06	6.6 ± 6.8	103.2	9.2e+05 ± 5.3e+05	9.1 ± 5.3	58.2
S29	7.4e+05 ± 8.1e+05	11.1 ± 12.2	109.1	5.4e+05 ± 3.5e+05	15.4 ± 9.8	64.1
S31	1.1e+06 ± 1.0e+06	7.8 ± 7.5	96.4	7.8e+05 ± 4.0e+05	10.7 ± 5.5	51.4
S33	1.8e+06 ± 1.9e+06	4.7 ± 5.0	107.0	1.3e+06 ± 7.9e+05	6.5 ± 4.0	62.0
S38	1.1e+05 ± 1.0e+05	76.9 ± 73.3	95.4	7.8e+04 ± 3.9e+04	106.0 ± 53.4	50.4
S39	2.5e+05 ± 2.5e+05	33.2 ± 32.8	98.8	1.8e+05 ± 9.7e+04	45.8 ± 24.6	53.8
S42	3.2e+06 ± 4.0e+06	2.6 ± 3.1	122.7	2.4e+06 ± 1.8e+06	3.5 ± 2.7	77.7
S54	1.9e+06 ± 3.5e+06	4.4 ± 8.4	188.3	1.4e+06 ± 1.9e+06	6.1 ± 8.8	143.3
S55	9.6e+04 ± 9.3e+04	86.5 ± 84.5	97.6	6.9e+04 ± 3.7e+04	119.3 ± 62.7	52.6
S60	6.6e+05 ± 6.4e+05	12.6 ± 12.3	97.7	4.8e+05 ± 2.5e+05	17.4 ± 9.2	52.7
S66	8.5e+06 ± 8.6e+06	1.0 ± 1.0	101.4	6.2e+06 ± 3.5e+06	1.3 ± 0.8	56.4
S67	5.2e+06 ± 5.2e+06	1.6 ± 1.6	100.1	3.8e+06 ± 2.1e+06	2.2 ± 1.2	55.1
S71	1.3e+06 ± 1.4e+06	6.4 ± 6.8	107.3	9.4e+05 ± 5.9e+05	8.8 ± 5.5	62.3
S83	7.6e+06 ± 8.4e+06	1.1 ± 1.2	110.3	5.5e+06 ± 3.6e+06	1.5 ± 1.0	65.3
S85	2.3e+07 ± 4.9e+07	0.4 ± 0.8	211.0	1.7e+07 ± 2.8e+07	0.5 ± 0.8	166.0
S87	2.0e+07 ± 2.1e+07	0.4 ± 0.4	102.4	1.5e+07 ± 8.5e+06	0.6 ± 0.3	57.4
S89	3.6e+06 ± 3.8e+06	2.3 ± 2.5	107.8	2.6e+06 ± 1.6e+06	3.2 ± 2.0	62.8
S91	1.2e+07 ± 1.2e+07	0.7 ± 0.7	101.9	8.4e+06 ± 4.8e+06	1.0 ± 0.6	56.9
S96	8.4e+06 ± 8.4e+06	1.0 ± 1.0	100.0	6.1e+06 ± 3.3e+06	1.4 ± 0.7	55.0
S97	1.5e+07 ± 1.9e+07	0.6 ± 0.7	125.9	1.1e+07 ± 8.8e+06	0.8 ± 0.6	80.9
S145	4.5e+06 ± 6.1e+06	1.9 ± 2.5	136.7	3.2e+06 ± 3.0e+06	2.6 ± 2.4	91.7
S175	8.2e+04 ± 9.0e+04	101.4 ± 111.8	110.3	5.9e+04 ± 3.9e+04	139.7 ± 91.2	65.3
R34	7.6e+06 ± 9.2e+06	1.1 ± 1.3	120.5	5.5e+06 ± 4.2e+06	1.5 ± 1.1	75.5
R44	3.3e+07 ± 5.2e+07	0.2 ± 0.4	156.2	2.4e+07 ± 2.7e+07	0.3 ± 0.4	111.2

**Table 3.** The same as in Table 2, but for  $f_{SP} = 1.16 \pm 0.16$  and  $f_{SP} = 1.144 \pm 0.144$ .

Star	$f_{SP} = 1.16 \pm 0.16$			$f_{SP} = 1.144 \pm 0.144$		
	$\lambda \pm \Delta\lambda$ (AU)	$m_g \pm \Delta m_g$ ( $10^{-24}$ eV)	R.E. (%)	$\lambda \pm \Delta\lambda$ (AU)	$m_g \pm \Delta m_g$ ( $10^{-24}$ eV)	R.E. (%)
S1	1.3e+06 ± 7.2e+05	6.4 ± 3.6	55.7	1.4e+06 ± 7.6e+05	6.1 ± 3.4	55.7
S2	5.2e+04 ± 2.7e+04	158.0 ± 81.0	51.3	5.5e+04 ± 2.8e+04	149.9 ± 76.8	51.3
S4	7.0e+05 ± 3.6e+05	11.9 ± 6.1	51.7	7.4e+05 ± 3.8e+05	11.3 ± 5.8	51.7
S6	7.9e+05 ± 4.0e+05	10.5 ± 5.3	50.2	8.3e+05 ± 4.2e+05	10.0 ± 5.0	50.2
S8	4.4e+05 ± 2.3e+05	18.9 ± 10.0	53.0	4.6e+05 ± 2.4e+05	17.9 ± 9.5	53.0
S9	3.5e+05 ± 1.9e+05	23.6 ± 12.9	54.7	3.7e+05 ± 2.0e+05	22.3 ± 12.2	54.7
S12	1.9e+05 ± 9.7e+04	44.1 ± 22.7	51.4	2.0e+05 ± 1.0e+05	41.8 ± 21.5	51.4
S13	4.3e+05 ± 2.2e+05	19.2 ± 9.7	50.5	4.6e+05 ± 2.3e+05	18.2 ± 9.2	50.5
S14	5.7e+04 ± 3.6e+04	144.3 ± 89.9	62.3	6.1e+04 ± 3.8e+04	136.9 ± 85.3	62.3
S17	6.9e+05 ± 3.6e+05	12.0 ± 6.3	52.1	7.3e+05 ± 3.8e+05	11.4 ± 5.9	52.1
S18	3.6e+05 ± 1.8e+05	23.3 ± 12.0	51.5	3.8e+05 ± 1.9e+05	22.1 ± 11.4	51.5
S19	7.4e+05 ± 5.3e+05	11.1 ± 8.0	71.4	7.8e+05 ± 5.6e+05	10.6 ± 7.5	71.4
S21	2.0e+05 ± 1.1e+05	42.2 ± 23.0	54.6	2.1e+05 ± 1.1e+05	40.0 ± 21.8	54.6
S22	4.7e+06 ± 3.2e+06	1.8 ± 1.2	69.1	4.9e+06 ± 3.4e+06	1.7 ± 1.2	69.1
S23	3.5e+05 ± 2.5e+05	23.4 ± 16.5	70.6	3.7e+05 ± 2.6e+05	22.2 ± 15.7	70.6
S24	1.0e+06 ± 5.8e+05	8.3 ± 4.8	58.2	1.1e+06 ± 6.1e+05	7.9 ± 4.6	58.2
S29	5.9e+05 ± 3.8e+05	14.1 ± 9.0	64.1	6.2e+05 ± 4.0e+05	13.4 ± 8.6	64.1
S31	8.5e+05 ± 4.3e+05	9.8 ± 5.0	51.4	8.9e+05 ± 4.6e+05	9.3 ± 4.8	51.4
S33	1.4e+06 ± 8.6e+05	6.0 ± 3.7	62.0	1.5e+06 ± 9.1e+05	5.6 ± 3.5	62.0
S38	8.5e+04 ± 4.3e+04	97.3 ± 49.0	50.4	9.0e+04 ± 4.5e+04	92.3 ± 46.5	50.4
S39	2.0e+05 ± 1.1e+05	42.0 ± 22.6	53.8	2.1e+05 ± 1.1e+05	39.8 ± 21.4	53.8
S42	2.6e+06 ± 2.0e+06	3.2 ± 2.5	77.7	2.7e+06 ± 2.1e+06	3.1 ± 2.4	77.7
S54	1.5e+06 ± 2.1e+06	5.6 ± 8.0	143.3	1.6e+06 ± 2.2e+06	5.3 ± 7.6	143.3
S55	7.6e+04 ± 4.0e+04	109.5 ± 57.6	52.6	8.0e+04 ± 4.2e+04	103.8 ± 54.6	52.6
S60	5.2e+05 ± 2.7e+05	16.0 ± 8.4	52.7	5.5e+05 ± 2.9e+05	15.2 ± 8.0	52.7
S66	6.7e+06 ± 3.8e+06	1.2 ± 0.7	56.4	7.1e+06 ± 4.0e+06	1.2 ± 0.7	56.4
S67	4.1e+06 ± 2.3e+06	2.0 ± 1.1	55.1	4.4e+06 ± 2.4e+06	1.9 ± 1.0	55.1
S71	1.0e+06 ± 6.4e+05	8.1 ± 5.0	62.3	1.1e+06 ± 6.8e+05	7.6 ± 4.8	62.3
S83	6.0e+06 ± 3.9e+06	1.4 ± 0.9	65.3	6.4e+06 ± 4.2e+06	1.3 ± 0.8	65.3
S85	1.8e+07 ± 3.0e+07	0.5 ± 0.8	166.0	1.9e+07 ± 3.2e+07	0.4 ± 0.7	166.0
S87	1.6e+07 ± 9.3e+06	0.5 ± 0.3	57.4	1.7e+07 ± 9.8e+06	0.5 ± 0.3	57.4
S89	2.8e+06 ± 1.8e+06	3.0 ± 1.9	62.8	3.0e+06 ± 1.9e+06	2.8 ± 1.8	62.8
S91	9.1e+06 ± 5.2e+06	0.9 ± 0.5	56.9	9.6e+06 ± 5.5e+06	0.9 ± 0.5	56.9
S96	6.6e+06 ± 3.6e+06	1.2 ± 0.7	55.0	7.0e+06 ± 3.8e+06	1.2 ± 0.7	55.0
S97	1.2e+07 ± 9.6e+06	0.7 ± 0.6	80.9	1.2e+07 ± 1.0e+07	0.7 ± 0.5	80.9
S145	3.5e+06 ± 3.2e+06	2.4 ± 2.2	91.7	3.7e+06 ± 3.4e+06	2.2 ± 2.0	91.7
S175	6.5e+04 ± 4.2e+04	128.2 ± 83.7	65.3	6.8e+04 ± 4.4e+04	121.6 ± 79.4	65.3
R34	6.0e+06 ± 4.6e+06	1.4 ± 1.0	75.5	6.4e+06 ± 4.8e+06	1.3 ± 1.0	75.5
R44	2.6e+07 ± 2.9e+07	0.3 ± 0.3	111.2	2.8e+07 ± 3.1e+07	0.3 ± 0.3	111.2

Although the current GRAVITY estimates of  $f_{SP} = 1.10 \pm 0.19$  (from [95]) and  $f_{SP} = 0.85 \pm 0.16$  and  $f_{SP} = 0.997 \pm 0.144$  (from [109]) can improve our previous constraints on the upper bound of graviton mass for  $\sim 30\%$  (these results can be compared with our previous corresponding estimates from Tables I and III in [55] for the corresponding

S-star), we have to stress that we made the assumption that  $f_{SP}$  has been measured for all S-star orbits already to a given precision. In reality, it is expected that the orbits of different S-stars should result with slightly different measured values and accuracies of  $f_{SP}$ . Because of this, our assumption that  $f_{SP}$  is the same for all S-stars (see Tables 2 and 3) probably does not hold.

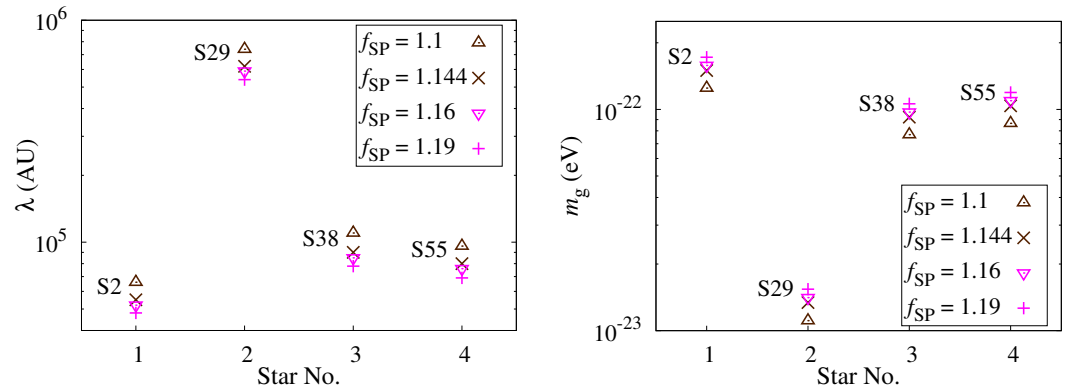


**Figure 2.** Left: Constraints on the Compton wavelength,  $\lambda$ , of the graviton from the orbits of the S2, S29, S38, and S55 stars, in cases of the following  $f_{SP}$  estimates: 1.1, 1.144, 1.16, and 1.19. Right: Upper bounds on graviton mass,  $m_g$ , for the same group of S-stars and the same  $f_{SP}$ .

#### PPN Fit of the Observed Orbit of the S2 Star

In order to verify the results presented in Tables 2 and 3, we also estimated the value of the Compton wavelength,  $\lambda$ , of the graviton by fitting the simulated orbits in the extended PPN<sub>γ</sub> formalism into the observed orbit of the S2 star. For this purpose, we used the publicly available astrometric observations of the S2 star from [85]. Orbital fitting in the frame of extended PPN<sub>γ</sub> formalism (7) was performed by minimization of the reduced  $\chi^2$  statistics,

$$\chi_{\text{red}}^2 = \frac{1}{2(N-\nu)} \sum_{i=1}^N \left[ \left( \frac{x_i^o - x_i^c}{\sigma_{xi}} \right)^2 + \left( \frac{y_i^o - y_i^c}{\sigma_{yi}} \right)^2 \right], \quad (16)$$

where  $(x_i^o, y_i^o)$  is the  $i$ -th observed position,  $(x_i^c, y_i^c)$  is the corresponding calculated position,  $N$  is the number of observations,  $\nu$  is number of unknown parameters, and  $\sigma_{xi}$  and  $\sigma_{yi}$  are the observed astrometric uncertainties.

The values of the graviton Compton wavelength,  $\lambda$ , SMBH mass,  $M$ , distance,  $R$ , to the GC, and the osculating orbital elements  $a, e, i, \Omega, \omega, P, T$ , which correspond to the minimum of  $\chi_{\text{red}}^2$ , were found using the differential evolution optimization method, implemented as Python Scipy function: [https://docs.scipy.org/doc/scipy/reference/generated/scipy.optimize.differential\\_evolution.html](https://docs.scipy.org/doc/scipy/reference/generated/scipy.optimize.differential_evolution.html) (accessed on 1 February 2024). This is a population-based metaheuristic search technique of finding the global minimum of a multivariate function, which is especially suitable in evolutionary computations since it is stochastic in nature, does not use gradient descent to find the minimum, can search large areas of candidate space, and seeks to iteratively enhances a candidate solution concerning a specified quality metric. In order to improve the minimization slightly, the final result of the differential evolution optimization is further enhanced at the end using Python Scipy function: <https://docs.scipy.org/doc/scipy/reference/generated/scipy.optimize.minimize.html> (accessed on 1 February 2024). This also results in an approximation for the inverse Hessian matrix of  $\chi_{\text{red}}^2$ , which, on the other hand, could be considered as a good estimation for the covariance matrix of the parameters. Therefore, the standard error for each fitted parameter can be calculated by taking the square root of the respective diagonal element of this covariance matrix.

A particular value of  $\chi_{\text{red}}^2$  that corresponds to some specific combination of the mentioned adjustable parameters is calculated in the following way:

1. First, a simulated orbit of the S2 star in the extended PPN<sub>γ</sub> formalism is calculated by numerical integration of the equations of motion (7), starting from initial conditions  $(x_0, y_0, \dot{x}_0, \dot{y}_0)$ , where the first two components specify the initial position and the last two the initial velocity in the orbital plane. In our simulations, the initial conditions correspond to the time of apocenter passage,  $t_{\text{ap}}$ , preceding the first astrometric observation at  $t_0$ :  $t_{\text{ap}} = T - (2k - 1)\frac{P}{2}$ , where  $T$  is the time of pericenter passage,  $P$  is the orbital period, and  $k$  is the smallest positive integer (number of periods) for which  $t_{\text{ap}} \leq t_0$ . Then, the initial conditions are:  $x_0 = -r_{\text{ap}}$ ,  $y_0 = 0$ ,  $\dot{x}_0 = 0$ , and  $\dot{y}_0 = -v_{\text{ap}}$ , where  $r_{\text{ap}} = a(1 + e)$  is the apocenter distance and  $v_{\text{ap}} = \frac{2\pi a}{P} \sqrt{\frac{1-e}{1+e}}$  is the corresponding orbital velocity at the apocenter.
2. The true orbit obtained in the first step, which depends only on  $a, e, P, T$ , was then projected to the observer's sky plane using the remaining geometrical orbital elements  $i, \Omega, \omega$ , in order to obtain the corresponding positions  $(x^c, y^c)$  along the apparent orbit,

$$x^c = Bx + Gy, \quad y^c = Ax + Fy, \quad (17)$$

where  $A, B, F$ , and  $G$  are the Thiele–Innes elements:

$$\begin{aligned} A &= \cos \Omega \cos \omega - \sin \Omega \sin \omega \cos i, \\ B &= \sin \Omega \cos \omega + \cos \Omega \sin \omega \cos i, \\ F &= -\cos \Omega \sin \omega - \sin \Omega \cos \omega \cos i, \\ G &= -\sin \Omega \sin \omega + \cos \Omega \cos \omega \cos i. \end{aligned} \quad (18)$$

In addition, the radial velocities,  $V_{\text{rad}}$ , are obtained from the corresponding true positions  $(x, y)$  and orbital velocities  $(\dot{x}, \dot{y})$  as (see, e.g., [62] and references therein)

$$V_{\text{rad}} = \frac{\sin i}{\sqrt{x^2 + y^2}} [\sin(\theta + \omega) \cdot (x\dot{x} + y\dot{y}) + \cos(\theta + \omega) \cdot (x\dot{y} - y\dot{x})], \quad (19)$$

where  $\theta = \arctan \frac{y}{x}$ .

3. Finally,  $\chi_{\text{red}}^2$  is obtained according to Equation (16), taking into account only those apparent positions  $(x^c, y^c)$  that are calculated at the same epochs as the astrometric observations  $(x^o, y^o)$ .

The obtained results of the orbital fitting in the case of the S2 star are presented in Figure 3, and the corresponding best-fit values of the parameters are provided in Table 4. As can be seen from Figure 3, and since the best fit resulted with  $\chi_{\text{red}}^2 = 1.108$ , which is only slightly larger than 1, the best-fit orbit of the S2 star in the extended PPN<sub>γ</sub> formalism is in very good agreement with the observations.

**Table 4.** Best-fit values of the graviton Compton wavelength,  $\lambda$ , SMBH mass,  $M$ , and distance,  $R$ , to the GC and the osculating orbital elements  $a, e, i, \Omega, \omega, P, T$  of the S2 star orbit.

Parameter	Value	Fit Error	Unit
$\lambda$	82,175.7	9828.05	AU
$M$	4.15	0.27	$10^6 M_{\odot}$
$R$	8.33	0.198	kpc
$a$	0.1229	0.00430	arcsec
$e$	0.8797	0.01597	
$i$	134.89	1.984	°
$\Omega$	224.57	5.208	°
$\omega$	62.78	4.562	°
$P$	15.98	0.362	yr
$T$	2018.12219	0.696709	yr

Concerning the graviton Compton wavelength,  $\lambda$ , obtained from the S2 star orbit, it can be seen that its best-fit value of  $\lambda \approx 8.2 \times 10^4$  AU from Table 4 is slightly larger, but still within the error intervals of the corresponding values from Tables 2 and 3, obtained according to Equation (14) from the detected values of  $f_{SP}$ . Therefore, the results of direct orbital fitting are in agreement with our constraints on the graviton Compton wavelength,  $\lambda$ , and mass,  $m_g$ , presented in Tables 2 and 3, which were obtained from the values of  $f_{SP}$  estimated by the GRAVITY Collaboration.

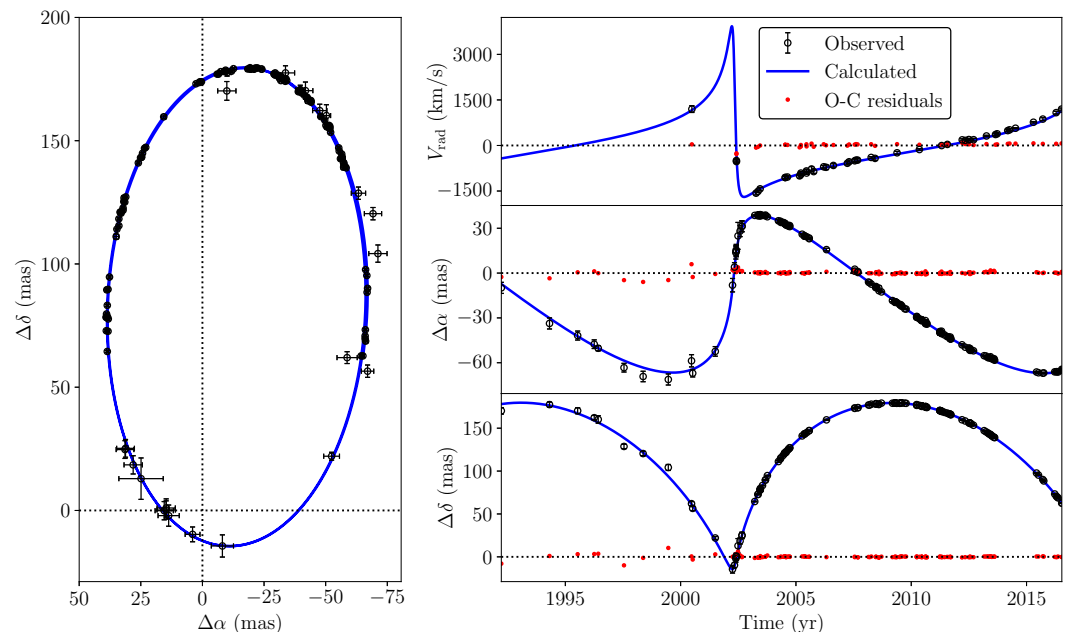


**Figure 3.** Left: Comparison between the best-fit orbit of the S2 star (blue solid line), simulated in the extended PPN $_{\gamma}$  formalism, and the corresponding astrometric observations from [85] (black circles with error bars). Right: The same for the radial velocity of the S2 star (top), as well as for its  $\alpha$  (middle) and  $\delta$  (bottom) offset relative to the position of Sgr A\* at the coordinate origin. Red dots in the right panels denote the corresponding O–C residuals.

## 5. Conclusions

Here we used the phenomenological Yukawa-like gravitational potential from [1,2] in order to obtain the constraints on the graviton mass,  $m_g$ , from the detected Schwarzschild precession in the observed stellar orbits around the SMBH at the GC. For this purpose, we used two modified/extended PPN formalisms in order to derive the relation between the Compton wavelength,  $\lambda$ , of the graviton and parameter  $f_{SP}$ , which parametrizes the effect of the Schwarzschild metric and was obtained by the GRAVITY Collaboration from the observed stellar orbits at the GC. The results from this study can be summarized as follows:

1. We found the condition for parameter  $\lambda$  of the phenomenological Yukawa-like gravitational potential (3) under which the orbital precession in this potential deviates from the Schwarzschild precession in GR by a factor  $f_{SP}$ ;
2. The relation (14) derived from the phenomenological potential (3) in the frame of the two modified/extended PPN formalisms could be used for obtaining the reliable constraints on the graviton mass,  $m_g$ , from the latest estimates for  $f_{SP}$  by the GRAVITY Collaboration in cases when  $f_{SP} > 1$ ;
3. Both of the studied PPN formalisms result in close and very similar simulated orbits of S-stars, which practically overlap during the first orbital period and then begin to slowly diverge over time due to some assumed theoretical approximations;
4. In most cases, the constraints on the upper bound on graviton mass,  $m_g$ , and its absolute error,  $\Delta m_g$ , obtained using the phenomenological potential (3), were improved by  $\sim 30\%$  in respect to our previous corresponding estimates from [55], obtained using

- a slightly different Yukawa-like potential derived in the frame of  $f(R)$  theories of gravity, although the relative errors in both cases remained the same;
5. These results were also confirmed in the case of the S2 star by fitting its observed orbit into the frame of the extended PPN<sub>γ</sub> formalism, which resulted in the best-fit value for the graviton Compton wavelength,  $\lambda$ , within the error intervals of its corresponding estimates obtained according to Equation (14) from the detected values of  $f_{SP}$ ;
  6. The least reliable constraints with unrealistically high uncertainties were only obtained from estimates for  $f_{SP}$  that were very close to its value predicted by GR, being only slightly larger than 1;
  7. If one compares the results from Table 2 with those from Table 3, it can be seen that the upper bounds on graviton mass,  $m_g$ , are very similar. In the case of the S2 star,  $m_g < (1.5 \pm 0.8) \times 10^{-22}$  eV and the relative error is approximately 50%. We can conclude that more precise future observations are required in order to further improve the upper graviton mass bounds.

**Author Contributions:** Methodology, P.J., V.B.J., D.B. and A.F.Z.; investigation, P.J., V.B.J., D.B. and A.F.Z.; writing—original draft preparation, P.J., V.B.J., D.B. and A.F.Z.; writing—review and editing, P.J., V.B.J., D.B. and A.F.Z. All coauthors participated in writing, calculation and discussion of obtained results. All authors have read and agreed to the published version of the manuscript.

**Funding:** This research was funded by the Ministry of Science, Technological Development and Innovations of the Republic of Serbia through the Project contracts No. 451-03-66/2024-03/200002 and 451-03-66/2024-03/200017.

**Data Availability Statement:** Data are contained within the article.

**Conflicts of Interest:** The authors declare no conflicts of interest.

### Abbreviations

The following abbreviations are used in this manuscript:

GC	Galactic Center
GR	General Relativity
SMBH	Supermassive Black Hole
PPN formalism	Parameterized Post-Newtonian formalism

### References

1. Will, C.M. Bounding the mass of the graviton using gravitational-wave observations of inspiralling compact binaries. *Phys. Rev. D* **1998**, *57*, 2061. [\[CrossRef\]](#)
2. Will, C.M. Solar system versus gravitational-wave bounds on the graviton mass. *Class. Quant. Grav.* **2018**, *35*, 17LT01. [\[CrossRef\]](#)
3. Fischbach, E.; Talmadge, C.L. *The Search for Non-Newtonian Gravity*; Springer: Heidelberg, Germany; New York, NY, USA, 1999; 305p.
4. Kopeikin, S.; Vlasov, I. Parametrized post-Newtonian theory of reference frames, multipolar expansions and equations of motion in the N-body problem. *Phys. Rep.* **2004**, *400*, 209. [\[CrossRef\]](#)
5. Clifton, T. *Alternative Theories of Gravity*; University of Cambridge: Cambridge, UK, 2006. [\[CrossRef\]](#)
6. Capozziello, S.; de Laurentis, M. Extended Theories of Gravity. *Phys. Rep.* **2011**, *509*, 167. [\[CrossRef\]](#)
7. Capozziello, S.; Faraoni, V. *Beyond Einstein Gravity: A Survey of Gravitational Theories for Cosmology and Astrophysics*; Fundamental Theories of Physics; Springer: Dordrecht, The Netherlands, 2011; Volume 170.
8. Nojiri, S.; Odintsov, S.D. Unified cosmic history in modified gravity: From F(R) theory to Lorentz non-invariant models. *Phys. Rept.* **2011**, *505*, 59. [\[CrossRef\]](#)
9. Capozziello, S.; Laurentis, M.D. The dark matter problem from  $f(R)$  gravity viewpoint. *Ann. Phys.* **2012**, *524*, 545. [\[CrossRef\]](#)
10. Clifton, T.; Ferreira, P.G.; Padilla, A.; Skordis, C. Modified gravity and cosmology. *Phys. Rep.* **2012**, *513*, 1.
11. Nojiri, S.; Odintsov, S.D.; Oikonomou, V.K. Modified Gravity Theories on a Nutshell: Inflation, Bounce and Late-time Evolution. *Phys. Rept.* **2017**, *692*, 1. [\[CrossRef\]](#)
12. Salucci, P.; Esposito, G.; Lambiase, G.; Battista, E.; Benetti, M.; Bini, D.; Boco, L.; Sharma, G.; Bozza, V.; Buoninfante, L.; et al. Einstein, Planck and Vera Rubin: Relevant encounters between the Cosmological and the Quantum Worlds. *Front. Phys.* **2021**, *8*, 603190. [\[CrossRef\]](#)
13. Fierz, M.; Pauli, W. On Relativistic Wave Equations for Particles of Arbitrary Spin in an Electromagnetic Field. *Proc. R. Soc. Lond. Ser. A* **1939**, *173*, 211.

14. Logunov, A.A.; Mestvirishvili, M.A.; Chugreev, Y.V. Graviton Mass and Evolution of a Friedmann Universe. *Theor. Math. Phys.* **1988**, *74*, 1. [[CrossRef](#)]
15. Chugreev, Y.V. Cosmological consequences of the relativistic theory of gravitation with massive gravitons. *Theor. Math. Phys.* **1989**, *79*, 554. [[CrossRef](#)]
16. Gershtein, S.S.; Logunov, A.A.; Mestvirishvili, M.A. Graviton Mass and the Total Relative Mass Density  $\Omega_{tot}$  in the Universe. *Dokl. Phys.* **2003**, *48*, 282. [[CrossRef](#)]
17. Gershtein, S.S.; Logunov, A.A.; Mestvirishvili, M.A.; Tkachenko, N.P. Graviton mass, quintessence, and oscillatory character of Universe evolution. *Phys. Atomic Nucl.* **2004**, *67*, 1596. [[CrossRef](#)]
18. Gershtein, S.S.; Logunov, A.A.; Mestvirishvili, M.A. Gravitational field self-limitation and its role in the Universe. *Phys.-Uspekhi* **2006**, *49*, 1179. [[CrossRef](#)]
19. Rubakov, V.A.; Tinyakov, P.G. Infrared-modified gravities and massive gravitons. *Phys. Usp.* **2008**, *51*, 759. [[CrossRef](#)]
20. Babichev, E.; Deffayet, C.; Ziour, R. Recovery of general relativity in massive gravity via the Vainshtein mechanism. *Phys. Rev. D* **2010**, *82*, 104008. [[CrossRef](#)]
21. de Rham, C.; Gabadadze, G.; Tolley, A.J. Resummation of Massive Gravity. *Phys. Rev. Lett.* **2011**, *89*, 231101. [[CrossRef](#)] [[PubMed](#)]
22. de Rham, C. Massive Gravity. *Living Rev. Relativ.* **2014**, *17*, 7. [[CrossRef](#)]
23. de Rham, C.; Deskins, J.T.; Tolley, A.J.; Zhou, S.-Y. Massive Gravity. *Rev. Mod. Phys.* **2017**, *89*, 025004. [[CrossRef](#)]
24. Boulware, D.G.; Deser, S. Can Gravitation Have a Finite Range? *Phys. Rev. D* **1972**, *6*, 3368. [[CrossRef](#)]
25. LIGO Scientific Collaboration and Virgo Collaboration; Abbott, B.P.; Abbott, R.; Abbott, T.; Abernathy, M.R.; Acernese, F.; Ackley, K.; Adams, C.; Adams, T.; Addesso, P.; et al. Observation of Gravitational Waves from a Binary Black Hole Merger. *Phys. Rev. Lett.* **2016**, *116*, 061102. [[CrossRef](#)] [[PubMed](#)]
26. LIGO Scientific Collaboration; Virgo Collaboration and KAGRA Collaboration; Abbott, R.; Abe, H.; Acernese, F.; Ackley, K.; Adhikari, N.; Adhikari, R.X.; Adkins, V.K.; Adya, V.B.; et al. Tests of General Relativity with GWTC-3. *arXiv* **2021**. arXiv:2112.06861.
27. Particle Data Group. Review of particle physics. *Progr. Theor. Exper. Phys.* **2022**, *2022*, 083C01. [[CrossRef](#)]
28. Poisson, E.; Will, C.M. *Gravity (Newtonian, Post-Newtonian, Relativistic)*; Cambridge University Press: Cambridge, UK, 2014; ISBN 978-1-107-03286-6.
29. Sanders, R.H. Anti-gravity and galaxy rotation curves. *Astron. Astrophys.* **1984**, *136*, L21.
30. Talmadge, C.; Berthias, J.-P.; Hellings, R.W.; Standish, E.M. Model-independent constraints on possible modifications of Newtonian gravity. *Phys. Rev. Lett.* **1988**, *61*, 1159. [[CrossRef](#)]
31. White, M.J.; Kochanek, C.S. Constraints on the long-range properties of gravity from weak gravitational lensing. *Astrophys. J.* **2001**, *560*, 539. [[CrossRef](#)]
32. Amendola, L.; Quercellini, C. Skewness as a test of the equivalence principle. *Phys. Rev. Lett.* **2004**, *92*, 181102. [[CrossRef](#)]
33. Reynaud, S.; Jaekel, M.-T. Testing the Newton law at long distances. *Int. J. Mod. Phys. A* **2005**, *20*, 2294. [[CrossRef](#)]
34. Sealfon, C.; Verde, L.; Jimenez, R. Limits on deviations from the inverse-square law on megaparsec scales. *Phys. Rev. D* **2005**, *71*, 083004. [[CrossRef](#)]
35. Moffat, J.W. Gravitational theory, galaxy rotation curves and cosmology without dark matter. *J. Cosmol. Astropart. P.* **2005**, *5*, 22. [[CrossRef](#)]
36. Moffat, J.W. Scalar tensor vector gravity theory. *J. Cosmol. Astropart. P.* **2006**, *03*, 004. [[CrossRef](#)]
37. Sereno, M.; Jetzer, P. Dark matter versus modifications of the gravitational inverse-square law: Results from planetary motion in the Solar system. *Mon. Not. R. Astron. Soc.* **2006**, *371*, 626. [[CrossRef](#)]
38. Capozziello, S.; Stabile, A.; Troisi, A. Newtonian limit of f(R) gravity. *Phys. Rev. D* **2007**, *76*, 104019. [[CrossRef](#)]
39. Iorio, L. Constraints on the range  $\Lambda$  of Yukawa-like modifications to the Newtonian inverse-square law of gravitation from Solar System planetary motions. *J. High Energy Phys.* **2007**, *10*, 41. [[CrossRef](#)]
40. Iorio, L. Putting Yukawa-like Modified Gravity (MOG) on the test in the Solar System. *Sch. Res. Exch.* **2008**, *2008*, 238385. [[CrossRef](#)]
41. Adelberger, E.G.; Gundlach, J.H.; Heckel, B.R.; Hoedl, S.; Schlamminger, S. Torsion balance experiments: A low-energy frontier of particle physics. *Prog. Part. Nucl. Phys.* **2009**, *62*, 102. [[CrossRef](#)]
42. Capozziello, S.; de Filippis, E.; Salzano, V. Modelling clusters of galaxies by f(R)-gravity. *Mon. Not. R. Astron. Soc.* **2009**, *394*, 947. [[CrossRef](#)]
43. Cardone, V.F.; Capozziello, S. Systematic biases on galaxy haloes parameters from Yukawa-like gravitational potentials. *Mon. Not. R. Astron. Soc.* **2011**, *414*, 1301. [[CrossRef](#)]
44. Miao, X.; Shao, L.; Ma, B.-Q. Bounding the mass of graviton in a dynamic regime with binary pulsars. *Phys. Rev. D* **2019**, *99*, 123015. [[CrossRef](#)]
45. Capozziello, S.; Altucci, C.; Bajardi, F.; Basti, A.; Beverini, N.; Carelli, G.; Ciampini, D.; Di Virgilio, A.D.; Fuso, F.; Giacomelli, U.; et al. Constraining theories of gravity by GINGER experiment. *Eur. Phys. J. Plus* **2021**, *136*, 394. [[CrossRef](#)]
46. De Martino, I.; della Monica, R.; De Laurentis, M. f(R)-gravity after the detection of the orbital precession of the S2 star around the Galactic centre massive black hole. *Phys. Rev. D* **2021**, *104*, L101502. [[CrossRef](#)]
47. della Monica, R.; De Martino, I.; De Laurentis, M. Constraining MOdified Gravity with the S2 star. *Universe* **2022**, *8*, 137. [[CrossRef](#)]

48. Benisty, D. Testing modified gravity via Yukawa potential in two body problem: Analytical solution and observational constraints. *Phys. Rev. D* **2022**, *106*, 043001. [[CrossRef](#)]
49. Dong, Y.; Shao, L.; Hu, Z.; Miao, X.; Wang, Z. Prospects for constraining the Yukawa gravity with pulsars around Sagittarius A\*. *J. Cosmol. Astropart. P.* **2022**, *11*, 51. [[CrossRef](#)]
50. Tan, Y.; Lu, Y. Constraining the Yukawa Gravity with Post Newtonian Approximation using S-star Orbits around the Supermassive Black Hole in our Galactic Center. *arXiv* **2024**, arXiv:2402.00333.
51. Borka, D.; Capozziello, S.; Jovanović, P.; Borka Jovanović, V. Probing hybrid modified gravity by stellar motion around Galactic Center. *Astropart. Phys.* **2016**, *79*, 41. [[CrossRef](#)]
52. Zakharov, A.F.; Jovanović, P.; Borka, D.; Borka Jovanović, V. Constraining the range of Yukawa gravity interaction from S2 star orbits II: Bounds on graviton mass. *J. Cosmol. Astropart. Phys.* **2016**, *5*, 45. [[CrossRef](#)]
53. Jovanović, P.; Borka, D.; Borka Jovanović, V.; Zakharov, A.F. Influence of bulk mass distribution on orbital precession of S2 star in Yukawa gravity. *Eur. Phys. J. D* **2021**, *75*, 145. [[CrossRef](#)]
54. Jovanović, P.; Borka Jovanović, V.; Borka, D.; Zakharov, A.F. Constraints on Yukawa gravity parameters from observations of bright stars. *J. Cosmol. Astropart. Phys.* **2023**, *3*, 056. [[CrossRef](#)]
55. Jovanović, P.; Borka Jovanović, V.; Borka, D.; Zakharov, A.F. Improvement of graviton mass constraints using GRAVITY's detection of Schwarzschild precession in the orbit of S2 star around the Galactic Center. *Phys. Rev. D* **2024**, *109*, 064046. [[CrossRef](#)]
56. Bernus, L.; Minazzoli, O.; Fienga, A.; Gastineau, M.; Laskar, J.; Deram, P. Constraining the Mass of the Graviton with the Planetary Ephemeris INPOP. *Phys. Rev. Lett.* **2019**, *123*, 161103. [[CrossRef](#)] [[PubMed](#)]
57. Clifton, T. Parametrized post-Newtonian limit of fourth-order theories of gravity. *Phys. Rev. D* **2008**, *77*, 24041. [[CrossRef](#)]
58. Alsing, J.; Berti, E.; Will, C.M.; Zaglauer, H. Gravitational radiation from compact binary systems in the massive Brans-Dicke theory of gravity. *Phys. Rev. D* **2012**, *85*, 064041. [[CrossRef](#)]
59. Gainutdinov, R.I. PPN Motion of S-Stars around Sgr A\*. *Astrophysics* **2020**, *63*, 470. [[CrossRef](#)]
60. Gainutdinov, R.; Baryshev, Y. Relativistic Effects in Orbital Motion of the S-Stars at the Galactic Center. *Universe* **2020**, *6*, 177. [[CrossRef](#)]
61. Borka, D.; Jovanović, P.; Borka Jovanović, V.; Zakharov, A.F. Constraints on  $R^n$  gravity from precession of orbits S2-like stars. *Phys. Rev. D* **2012**, *85*, 124004. [[CrossRef](#)]
62. Borka, D.; Jovanović, P.; Borka Jovanović, V.; Zakharov, A.F. Constraining the range of Yukawa gravity interaction from S2 star orbits. *J. Cosmol. Astropart. Phys.* **2013**, *11*, 50. [[CrossRef](#)]
63. Zakharov, A.F.; Borka, D.; Borka Jovanović, V.; Jovanović, P. Constraints on  $R^n$  gravity from precession of orbits of S2-like stars: A case of a bulk distribution of mass. *Adv. Space Res.* **2014**, *54*, 1108. [[CrossRef](#)]
64. Capozziello, S.; Borka, D.; Jovanović, P.; Borka Jovanović, V.B. Constraining Extended Gravity Models by S2 star orbits around the Galactic Centre. *Phys. Rev. D* **2014**, *90*, 44052. [[CrossRef](#)]
65. Zakharov, A.F.; Jovanović, P.; Borka, D.; Borka Jovanović, V. Constraining the range of Yukawa gravity interaction from S2 star orbits III: Improvement expectations for graviton mass bounds. *J. Cosmol. Astropart. Phys.* **2018**, *4*, 50. [[CrossRef](#)]
66. Dialektopoulos, K.F.; Borka, D.; Capozziello, S.; Borka Jovanović, V.; Jovanović, P. Constraining nonlocal gravity by S2 star orbits. *Phys. Rev. D* **2019**, *99*, 044053. [[CrossRef](#)]
67. Borka Jovanović, V.; Jovanović, P.; Borka, D.; Capozziello, S.; Gravina, S.; D'Addio, A. Constraining scalar-tensor gravity models by S2 star orbits around the Galactic Center. *Facta Univ. Ser. Phys. Chem. Technol.* **2019**, *17*, 11. [[CrossRef](#)]
68. Borka, D.; Borka Jovanović, V.; Capozziello, S.; Zakharov, A.F.; Jovanović, P. Estimating the Parameters of Extended Gravity Theories with the Schwarzschild Precession of S2 Star. *Universe* **2021**, *7*, 407. [[CrossRef](#)]
69. Zakharov, A.F. Testing the Galactic Centre potential with S-stars. *Mon. Not. R. Astron. Soc. Lett.* **2022**, *511*, L35. [[CrossRef](#)]
70. Zakharov, A.F. Orbits of Bright Stars Near the Galactic Center as a Tool to Test Gravity Theories. *Mosc. Univ. Phys. Bull.* **2022**, *77*, 341. [[CrossRef](#)]
71. Zakharov, A.F. Trajectories of Bright Stars and Shadows around Supermassive Black Holes as Tests of Gravity Theories. *Phys. Part. Nucl.* **2023**, *54*, 889. [[CrossRef](#)]
72. Borka, D.; Borka Jovanović, V.; Nikolić, V.N.; Lazarov, N.D.; Jovanović, P. Estimating the parameters of Hybrid Palatini gravity model with the Schwarzschild precession of S2, S38 and S55 stars: Case of bulk mass distribution. *Universe* **2022**, *8*, 70. [[CrossRef](#)]
73. Lynden-Bell, D.; Rees, M.J. The Galactic Center. *Mon. Not. R. Astron. Soc.* **1971**, *152*, 461. [[CrossRef](#)]
74. Oort, J.H. The Galactic Center. *Annu. Rev. Astron. Astrophys.* **1977**, *15*, 295. [[CrossRef](#)]
75. Rees, M.J. The Compact Source at the Galactic Center. *AIP Conf. Proc.* **1982**, *83*, 166.
76. Genzel, R.; Townes, C.H. Physical conditions, dynamics, and mass distribution in the center of the Galaxy. *Ann. Rev. Astron. Astrophys.* **1987**, *25*, 377. [[CrossRef](#)]
77. Townes, C. H.; Genzel, R. What is Happening at the Center of Our Galaxy? *Sci. Am.* **1990**, *262*, 46. [[CrossRef](#)]
78. Ghez, A.M.; Morris, M.; Becklin, E.E.; Tanner, A.; Kremenek, T. The accelerations of stars orbiting the Milky Way's central black hole. *Nature* **2000**, *407*, 349. [[CrossRef](#)] [[PubMed](#)]
79. Schodel, R.; Ott, T.; Genzel, R.; Hofmann, R.; Lehnert, M.; Eckart, A.; Mouawad, N.; Alexander, T.; Reid, M.J.; Lenzen, R.; et al. Closest star seen orbiting the supermassive black hole at the Centre of the Milky Way. *Nature* **2002**, *419*, 694. [[CrossRef](#)] [[PubMed](#)]

80. Ghez, A.M.; Salim, S.; Weinberg, N.N.; Lu, J.R.; Do, T.; Dunn, J.K.; Matthews, K.; Morris, M.R.; Yelda, S.; Becklin, E.E.; et al. Measuring distance and properties of the Milky Way's central supermassive black hole with stellar orbits. *Astrophys. J.* **2008**, *689*, 1044. [[CrossRef](#)]
81. Gillessen, S.; Eisenhauer, F.; Fritz, T.K.; Bartko, H.; Dodds-Eden, K.; Pfuhl, O.; Ott, T.; Genzel, R. The orbit of the star S2 around Sgr A\* from very large telescope and Keck data. *Astrophys. J.* **2009**, *707*, L114. [[CrossRef](#)]
82. Gillessen, S.; Eisenhauer, F.; Trippe, S.; Alexander, T.; Genzel, R.; Martins, F.; Ott, T. Monitoring stellar orbits around the massive black hole in the Galactic Center. *Astrophys. J.* **2009**, *692*, 1075. [[CrossRef](#)]
83. Genzel, R.; Eisenhauer, F.; Gillessen, S. The Galactic Center massive black hole and nuclear star cluster. *Rev. Mod. Phys.* **2010**, *82*, 3121. [[CrossRef](#)]
84. Meyer, L.; Ghez, A.M.; Schödel, R.; Yelda, S.; Boehle, A.; Lu, J.R.; Do, T.; Morris, M.R.; Becklin, E.E.; Matthews, K. The Shortest-Known-Period Star Orbiting Our Galaxy's Supermassive Black Hole. *Science* **2012**, *338*, 84. [[CrossRef](#)]
85. Gillessen, S.; Plewa, P.M.; Eisenhauer, F.; Sari, R.E.; Waisberg, I.; Habibi, M.; Pfuhl, O.; George, E.; Dexter, J.; von Fellenberg, S.; et al. An Update on Monitoring Stellar Orbits in the Galactic Center. *Astrophys. J.* **2017**, *837*, 30. [[CrossRef](#)]
86. Hees, A.; Do, T.; Ghez, A.M.; Martinez, G.D.; Naoz, S.; Becklin, E.E.; Boehle, A.; Chappell, S.; Chu, D.; Dehghanfar, A.; et al. Testing General Relativity with Stellar Orbits around the Supermassive Black Hole in Our Galactic Center. *Phys. Rev. Lett.* **2017**, *118*, 211101. [[CrossRef](#)]
87. Hees, A.; Ghez, A.M.; Do, T.; Lu, J.R.; Morris, M.R.; Becklin, E.E.; Witzel, G.; Boehle, A.; Chappell, S.; Chen, Z.; et al. Testing the gravitational theory with short-period stars around our Galactic Center. In Proceedings of the 52th Rencontres de Moriond, 2017 Gravitation, La Thuile, Italy, 25 March–1 April 2017; Auge, E., Dumarchez, J., Van, J.T.T., Eds.; ARISF: Lausanne, Switzerland, 2017; pp. 283–286. Available online: [https://moriond.in2p3.fr/Proceedings/2017/Moriond\\_Gravitation\\_2017.pdf](https://moriond.in2p3.fr/Proceedings/2017/Moriond_Gravitation_2017.pdf) (accessed on 1 February 2024).
88. Chu, D.S.; Do, T.; Hees, A.; Naoz, S.; Witzel, G.; Sakai, S.; Chappell, S.; Gautam, A.K.; Lu, J.R.; et al. Investigating the Binarity of S0-2: Implications for Its Origins and Robustness as a Probe of the Laws of Gravity around a Supermassive Black Hole. *Astrophys. J.* **2018**, *854*, 12. [[CrossRef](#)]
89. GRAVITY Collaboration; Abuter, R.; Amorim, A.; Anugu, N.; Bauböck, M.; Benisty, M.; Berger, J.P.; Blind, N.; Bonnet Brandner, W.; Buron, A.; et al. Detection of the gravitational redshift in the orbit of the star S2 near the Galactic centre massive black hole. *Astron. Astrophys.* **2018**, *615*, L15.
90. GRAVITY Collaboration; Abuter, R.; Amorim, A.; Bauböck, M.; Berger, J.P.; Bonnet, H.; Brandner, W.; Clénet, Y.; Du Foresto, V.C.; et al. A geometric distance measurement to the Galactic center black hole with 0.3% uncertainty. *Astron. Astrophys.* **2019**, *625*, L10.
91. Do, T.; Hees, A.; Ghez, A.; Martinez, G.D.; Chu, D.S.; Jia, S.; Sakai, S.; Lu, J.R.; Gautam, A.K.; O'Neil, K.K.; et al. Relativistic redshift of the star S0-2 orbiting the Galactic Center supermassive black hole. *Science* **2019**, *365*, 664. [[CrossRef](#)]
92. GRAVITY Collaboration. Scalar field effects on the orbit of S2 star. *Mon. Not. R. Astron. Soc.* **2019**, *489*, 4606. [[CrossRef](#)]
93. Saida, H.; Nishiyama, S.; Ohgami, T.; Takamori, Y.; Takahashi, M.; Minowa, Y.; Najarro, F.; Hamano, S.; Omiya, M.; Iwamatsu, A.; et al. A significant feature in the general relativistic time evolution of the redshift of photons coming from a star orbiting Sgr A\*. *Astron. Soc. Japan* **2019**, *71*, 126. [[CrossRef](#)]
94. Hees, A.; Do, T.; Roberts, B.M.; Ghez, A.M.; Nishiyama, S.; Bentley, R.O.; Gautam, A.K.; Jia, S.; Kara, T.; Lu, J.R.; et al. Search for a Variation of the Fine Structure Constant around the Supermassive Black Hole in Our Galactic Center. *Phys. Rev. Lett.* **2020**, *124*, 81101. [[CrossRef](#)]
95. GRAVITY Collaboration; Abuter, R.; Amorim, A.; Bauböck, M.; Berger, J.P.; Bonnet, H.; Brandner, W.; Cardoso, V.; Clénet, Y.; de Zeeuw, P.T.; et al. Detection of the Schwarzschild precession in the orbit of the star S2 near the Galactic centre massive black hole. *Astron. Astrophys.* **2020**, *636*, L5.
96. Genzel, R. Nobel Lecture: A forty-year journey. *Rev. Mod. Phys.* **2022**, *94*, 020501. [[CrossRef](#)]
97. Dokuchaev, V.I.; Eroshenko, Y.N. Physical laboratory at the center of the Galaxy. *Phys. Uspekhi* **2015**, *58*, 772. [[CrossRef](#)]
98. De Martino, I.; Lazkoz, R.; De Laurentis, M. Analysis of the Yukawa gravitational potential in  $f(R)$  gravity I: Semiclassical periastron advance. *Phys. Rev. D* **2018**, *97*, 104067. [[CrossRef](#)]
99. De Laurentis, M.; De Martino, I.; Lazkoz, R. Analysis of the Yukawa gravitational potential in  $f(R)$  gravity II: Relativistic periastron advance. *Phys. Rev. D* **2018**, *97*, 104068. [[CrossRef](#)]
100. Kalita, S. The Galactic Center Black Hole, Sgr A\*, as a Probe of New Gravitational Physics with the Scalaron Fifth Force. *Astrophys. J.* **2020**, *893*, 31. [[CrossRef](#)]
101. Lalremruati, P.C.; Kalita, S. Periastron shift of compact stellar orbits from general relativistic and tidal distortion effects near Sgr A\*. *Mon. Not. R. Astron. Soc.* **2021**, *502*, 3761. [[CrossRef](#)]
102. D'Addio, A. S-star dynamics through a Yukawa-like gravitational potential. *Phys. Dark Universe* **2021**, *33*, 100871. [[CrossRef](#)]
103. Lalremruati, P.C.; Kalita, S. Is It Possible to See the Breaking Point of General Relativity near the Galactic Center Black Hole? Consideration of Scalaron and Higher-dimensional Gravity. *Astrophys. J.* **2022**, *925*, 126. [[CrossRef](#)]
104. Benisty, D.; Davis, A.-C. Dark energy interactions near the Galactic Center. *Phys. Rev. D* **2022**, *105*, 024052. [[CrossRef](#)]
105. Benisty, D.; Mifsud, J.; Levi Said, J.; Staicova, D. Strengthening extended gravity constraints with combined systems:  $f(R)$  bounds from cosmology and the galactic center. *Phys. Dark Universe* **2023**, *42*, 101344. [[CrossRef](#)]

106. Bambhaniya, P.; Joshi, A.B.; Dey, D.; Joshi, P.S.; Mazumdar, A.; Harada, T.; Nakao, K.I. Relativistic orbits of S2 star in the presence of scalar field. *Eur. Phys. J. C* **2024**, *84*, 124. [[CrossRef](#)]
107. Will, C.M. *Theory and Experiment in Gravitational Physics*; Cambridge University Press: Cambridge, UK, 2018; 360p.
108. Will, C.M. The Confrontation between General Relativity and Experiment. *Living Rev. Relativ.* **2014**, *17*, 4. [[CrossRef](#)] [[PubMed](#)]
109. GRAVITY Collaboration; Abuter, R.; Aymar, N.; Amorim, A.; Ball, J.; Bauböck, M.; Berger, J.P.; Bonnet, H.; Bourdarot, G.; Brandner, W.; et al. Mass distribution in the Galactic Center based on interferometric astrometry of multiple stellar orbits. *Astron. Astrophys.* **2022**, *657*, L12.

**Disclaimer/Publisher's Note:** The statements, opinions and data contained in all publications are solely those of the individual author(s) and contributor(s) and not of MDPI and/or the editor(s). MDPI and/or the editor(s) disclaim responsibility for any injury to people or property resulting from any ideas, methods, instructions or products referred to in the content.